赵盼捞, 袁顺达, 原垭斌. 湘南魏家钨矿区祥林铺岩体锆石LA−MC−ICP−MS U−Pb测年——对南岭西端晚侏罗世钨矿成岩成矿作用的指示[J]. 中国地质, 2016, 43(1): 120−131.
Zhao Panlao, Yuan Shunda, Yuan Yabin. Zircon LA−MC−ICP−MS U−Pb dating of the Xianglinpu granites from the Weijia tungsten deposit in southern Hunan Province and its implications for the Late Jurassic tungsten metallogenesis in the westernmost Nanling W−Sn metallogenic belt[J]. Geology in China, 2016, 43(1): 120−131(in Chinese with English abstract).

湘南魏家钨矿区祥林铺岩体锆石LA−MC−ICP−MS U−Pb测年——对南岭西端晚侏罗世钨矿成岩成矿作用的指示

赵盼捞[1] 袁顺达[1] 原垭斌[2]
(1. 中国地质科学院矿产资源研究所, 国土资源部成矿作用与矿产资源评价重点实验室, 北京 100037;
2. 中国地质大学(北京) 地球科学与资源学院, 北京 100083)

提要: 魏家钨矿床位于湘南西部铜山岭地区, 是近年来在南岭成矿带西端新发现的一超大型矽卡岩型钨矿床。矿体主要产于祥林铺花岗岩与其围岩的接触带内, 其形成与祥林铺花岗岩密切相关。为厘清其成岩成矿时代, 本文对魏家钨矿区的花岗斑岩和石英斑岩进行了锆石LA−MC−ICP−MS U−Pb测年。结果显示, 矿区花岗斑岩侵位时间为(157.8±0.9) Ma (MSWD=1.06), 石英斑岩侵位时间为(158.3±1.4) Ma(MSWD=0.2)。矿区内花岗斑岩与石英斑岩侵位时间在误差范围内一致, 表明两者可能是同一岩浆演化至不同阶段的产物, 矿区内花岗质岩浆活动与钨多金属成矿作用时限约为158 Ma, 为南岭地区中生代"大规模成矿"作用(160~150 Ma)的组成部分。另外, 花岗斑岩中捕获有少量加里东期的岩浆锆石(435 Ma), 指示该区曾发生加里东期岩浆活动, 这与华南地区广泛存在的加里东期构造岩浆活动事件吻合。魏家钨矿成岩成矿时代的厘定对于在南岭成矿带西端寻找晚侏罗世钨矿具有重要的指示意义。

关 键 词: 花岗岩; 锆石U−Pb定年; 湘南; 魏家钨矿
中图分类号: P597.3; P588.12^{+}1; P618.67 **文献标志码**: A **文章编号**: 1000−3657(2016)01−0120−12

Zircon LA−MC−ICP−MS U−Pb dating of the Xianglinpu granites from the Weijia tungsten deposit in southern Hunan Province and its implications for the Late Jurassic tungsten metallogenesis in the westernmost Nanling W−Sn metallogenic belt

ZHAO Pan−lao[1], YUAN Shun−da[1], YUAN Ya−bin[2]
(1. *MLR Key Laboratory of Metallogeny and Mineral Assessment, Institute of Mineral Resources,*

收稿日期:2014−12−08;**改回日期**:2015−03−10
基金项目:国家重点基础研究"973"项目(2012CB416704)、国家自然科学基金项目(41173052、41373047、40903020)和中央级公益性科研院所基本业务费专项资金(K1204)联合资助。
作者简介:赵盼捞,男,1991年生,硕士,矿物学、岩石学、矿床学专业;E−mail: panlaozhao@163.com。
通讯作者:袁顺达,男,1980年生,博士,副研究员,矿床地球化学专业;E−mail: shundayuan@cags.ac.cn。

Chinese Academy of Geological Sciences, Beijing 100037, *China;*
2. *School of Earth Sciences and Mineral Resources, China University of Geosciences, Beijing* 100083, *China*)

Abstract: The Weijia tungsten deposit, located in the Tongshanling area of western Nanling metallogenic belt, is a newly discovered giant skarn tungsten deposit, with its orebodies mainly occurring at the contact zone between the Xianglinpu granite and Devonian carbonate rock. To determine the timing of the emplacement of the Xianglinpu granite and associated mineralization, the authors collected two kinds of granite, i.e., granite porphyry and quartz porphyry, from the Xianglingpu pluton for zircon LA−MC−ICP−MS U−Pb dating. The results show that the zircon U−Pb ages of granite porphyry and quartz porphyry are (157.8 ± 0.9) Ma (MSWD= 1.06) and (158.3 ± 1.4) Ma (MSWD=0.2), respectively, suggesting that their emplacements were coeval within error and they were derived from the same magma source. In addition, the captured zircons from granite porphyry yielded the weighed mean U−Pb age of (435.0 ± 3.1) Ma (MSWD=0.6), which recorded the Caledonian tectonic−magmatic event in this area. Based on the contact relationship between skarn tungsten orebodies and granite, the authors hold that the emplacement of Xianglinpu granite and associated tungsten mineralization occurred at ca.158 Ma, which coincided well with the large−scale mineralization of the Nanling in Middle−Late Jurassic (150−160) Ma. The constraint of the Late Jurassic Weijia skarn−type tungsten deposit implies the great potential of the late Jurassic skarn−type tungsten mineralization in western Nanling W−Sn metallogenic belt.

Key words: granite; U−Pb zircon dating; southern Hunan Province; Weijia tungsten deposit

About the first author: ZHAO Pan−lao, male, born in 1991, master; engages in the study of geology and geochemistry of ore deposits；E−mail: panlaozhao@163.com.

About the corresponding author: YUAN Shun−da, male, born in 1980, doctor, associate researcher, long engages in the study of geochronology and geochemistry of ore deposit; E−mail: shundayuan@cags.ac.cn.

Foud support: Supported by National Key Basic Research Program of China (973 Program) (No. 2012CB416704), National Natural Science Foundation of China (No. 41173052, 41373047, 40903020), and special fund for basic scientific search business of central public research institutes (K1204).

铜山岭地区位于NE向钦杭铜多金属成矿带与EW向南岭钨锡成矿带的叠合部位, 因而具有良好的成矿条件。长期以来, 该区以产出与花岗闪长(斑)岩有关的矽卡岩型Cu− (Mo) −Pb−Zn矿床为特征, 如铜山岭矽卡岩型Cu−(Pb−Zn−Ag)矿、庵堂岭矽卡岩型Pb−Zn矿、玉龙矽卡岩型Mo矿等[1]。魏家钨矿是该区新近发现的一个超大型矽卡岩型白钨矿床(333+334钨资源量达26万t)[1], 与该区矽卡岩型Cu−Pb−Zn矿主要与花岗闪长斑岩有关不同, 魏家钨矿床空间上主要产出于祥林铺花岗岩与泥盆纪碳酸盐岩的接触带。目前, 针对该矿的研究还很少, 仅有少量关于矿床地质特征及成矿机制等方面的研究[2−3]。精确厘定该矿成岩成矿时代对于理解区内多金属成矿及南岭地区中晚侏罗世钨锡矿床的时空分布格局具有重要意义。本次研究在已有研究及野外地质调查的基础上, 对祥林铺岩体开展锆石LA−MC−ICP−MS U−Pb测年, 为明确区内成岩成矿作用提供年代学依据, 并在此基础上进一步讨论南岭地区钨锡矿床时空分布规律。

1　区域地质概况

湘南钨锡矿集区构造位置处于扬子地块和华夏地块的对接带附近, 同时位于华南EW向南岭成矿带与NE向钦杭成矿带的结合部位。由于其特殊的大地构造位置, 且长期以来经历的多期次复杂的构造岩浆活动, 该区发育了一系列花岗岩体, 并相伴产出了一系列钨锡铅锌铜钼多金属矿床, 构成了一个大型多金属矿集区[4−10]。魏家钨矿床位于南岭成矿带西段, 在构造上处于水口山—铜山岭北东向断裂与都庞岭—祥林铺—九嶷山东西向基底断裂、怀化—道县北西向基底断裂的交汇部位(图1)。区域上除志留系、侏罗系和古近—新近系缺失外, 从寒武系至第四系均有出露。寒武—奥陶纪浅海相碎屑岩夹火山碎屑岩、硅质岩及不纯的碳酸盐岩构成该区基底, 厚达万余米。泥盆—三叠纪浅海相碳酸盐岩夹滨海或海陆交互相碎屑岩和白垩纪陆相碎屑岩构成区内盖层, 其中泥盆纪碳酸盐岩为钨矿主要赋存层位。除基底断裂外, 盖层构造主要为近

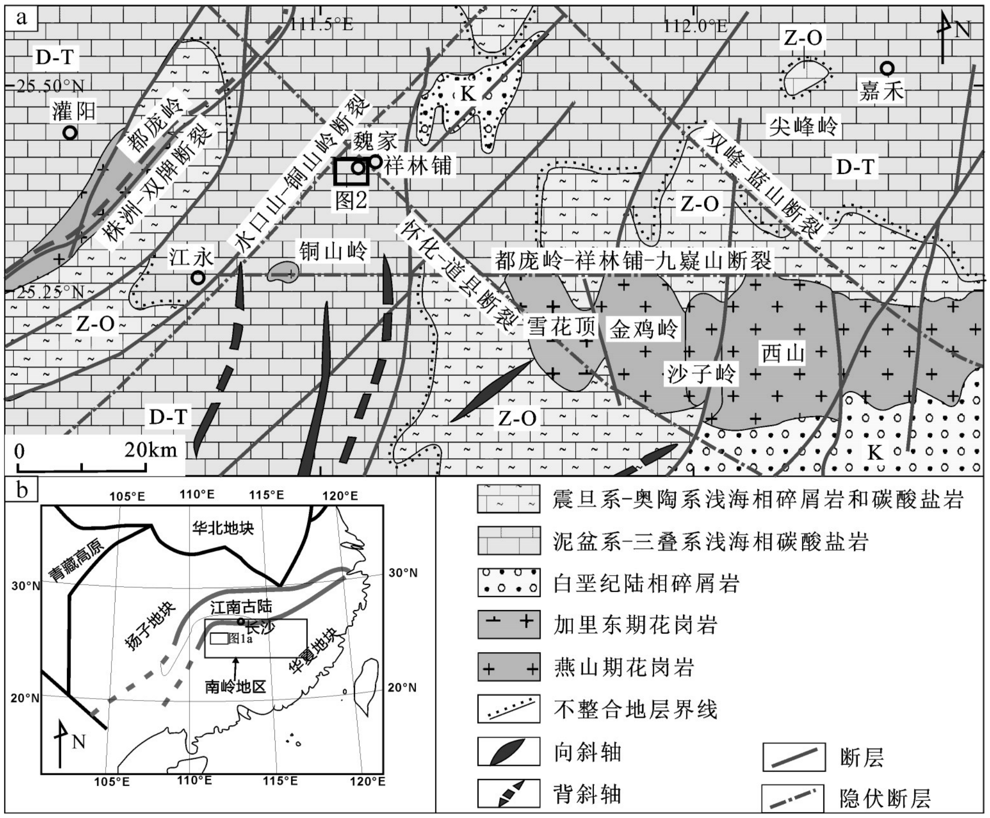

图1 铜山岭地区地质略图(据文献[2]修改)
Fig.1 Geological sketch map of Tongshanling area (modified after reference [2])

南北向褶皱断裂带,由侏罗山式皱褶及同轴向断裂组成[2]。区内岩浆岩较发育,多为复式岩体,主要为加里东期至燕山期的花岗岩和花岗闪长岩,主要有都庞岭岩体、铜山岭岩体、祥林铺岩体、雪花顶岩体、金鸡岭岩体、西山岩体等,岩体受到基底断裂的影响呈近东西向分布。

2　矿区地质

矿区内主要出露泥盆纪地层,自老至新依次为棋梓桥组、长龙界组和锡矿山组,岩性为一套滨—浅海相碳酸盐岩、碎屑岩及陆相碎屑岩。棋梓桥组为主要赋矿层位(图2),可以分为三段:下段主要为灰岩、白云质灰岩,厚200 m左右;中段主要为一套含生物碎屑白云质灰岩、白云岩,富含有机质和生物碎屑,化学性质活泼,有利含矿热液的贯通和交代,为层间矽卡岩型钨矿的重要赋存层位,上段为灰岩、白云质灰岩,厚150~200 m[2]。矿区内构造复杂,岩体和矿体受区内一近南北向背斜控制(图2)。背斜长约3000 m,宽约500 m,西翼较平缓,东翼较陡,祥林铺岩体侵位于该向斜轴部附近[2]。

魏家钨矿床产于祥林铺花岗岩与泥盆纪碳酸盐岩、碎屑岩接触带及其附近(图2)。矿体呈似层状隐伏产出(图3),分布于地表500 m以下,厚达139.73 m,主要赋存于矽卡岩、花岗斑岩以及大理岩中,以矽卡岩中最富,品位最高,表明钨矿化与祥林铺花岗岩关系密切[2]。矿化类型较多,主要有层间矽卡岩型钨矿、斑岩型钨矿、接触带型矽卡岩型钨矿、层间矽卡岩型铜矿等,其中以层间矽卡岩型钨矿规模最大最具找矿潜力[2]。区内围岩蚀变种类较多,以矽卡岩化最发育,与成矿关系最密切,其次为大理岩化、蛇纹石化、绢云母化、高岭土化、碳酸盐化等。矿石类型主要有矽卡岩型白钨矿、斑岩型白钨矿、矽卡岩型铜矿,矿石结构主要为他形粒状变晶结构、交代残余结构,构造主要为浸染状构造、条

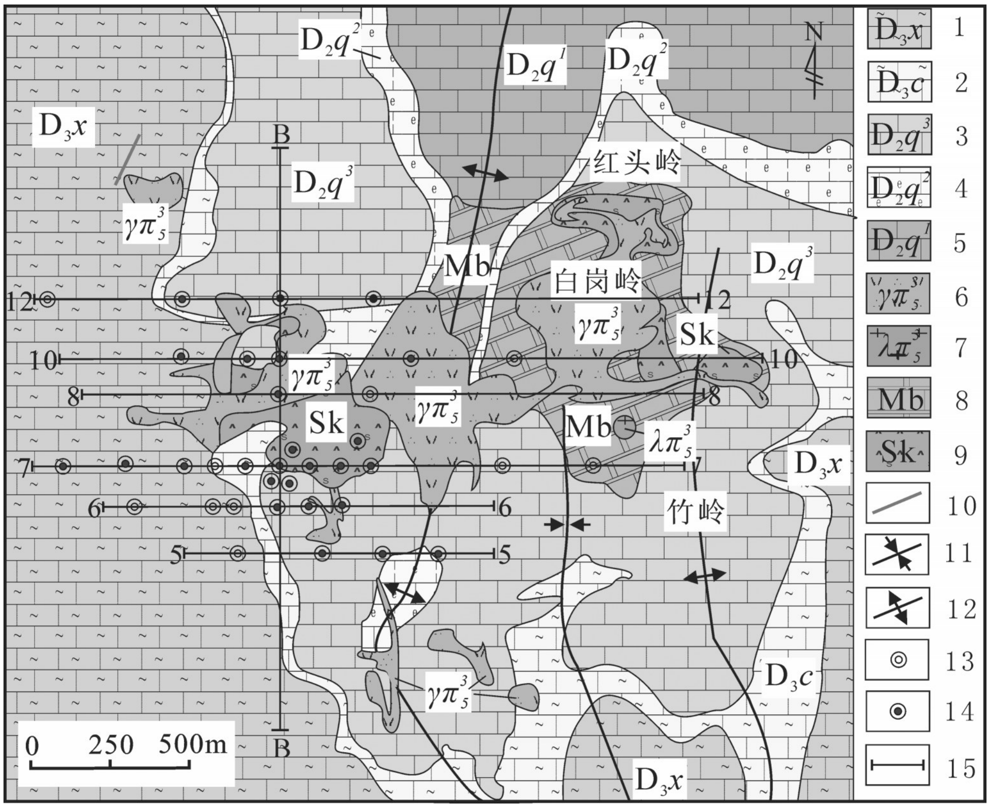

图2 魏家钨矿床矿区地质略图(据文献[3]修改)

1—上泥盆统锡矿山组; 2—上泥盆统长龙界组; 3—中泥盆统棋梓桥组上段; 4—中泥盆统棋梓桥组中段; 5—中泥盆统棋梓桥组下段; 6—花岗斑岩; 7—石英斑岩; 8—大理岩; 9—矽卡岩; 10—断层; 11—背斜轴线; 12—向斜轴线; 13—未见矿钻孔; 14—见矿钻孔; 15—勘探线及编号

Fig.2 Geological sketch map of the Weijia W deposit (modified after reference [3])

1−Upper Devonian Xikuangshan Formation; 2−Upper Devonian Changlongjie Formation; 3−Upper member of Middle Devonian Qiziqiao Formation; 4−Middle member of Middle Devonian Qiziqiao Formation; 5− Lower member of Middle Devonian Qiziqiao Formation; 6−Granite porphyry; 7−Quartz porphyry; 8−Marble; 9−Skarn; 10−Fault; 11−Anticline; 12−Syncline; 13−Barren drill hole; 14−Ore−intersecting drill hole; 15−Exploration line and its serial number

带状构造、块状构造等。

3　岩石岩相学特征

祥林铺岩体位于铜山岭岩体北东11~13 km处,为由30多个近东西向排列产出的小岩体组成的斑岩脉群,单个岩体出露面积数百平方米至0.35 km^{2}不等,岩性稳定。侵入体主体为花岗斑岩,岩体长0.8~1 km,宽0.2~0.5 km,面积近0.35 km,平面形态好似近东西向的猪腰型,岩体南侧出露少量石英斑岩[2]。经手标本和显微镜下鉴定本次实验所采样品为花岗斑岩(XLP−1)和石英斑岩(XLP−2)(图4)。花岗斑岩呈浅灰色,全晶质花岗斑状结构,块状构造。斑晶含量约为30%,主要为钾长石(15%)、斜长石(5%)、石英(10%)。斑晶粒度为0.5~1 mm,石英呈他形粒状,一级橙黄干涉色,钾长石和斜长石蚀变强烈,大部分蚀变为粘土矿物。基质为显微花岗结构,矿物组成为石英(23%~25%)、钾长石(30%)、斜长石(10%)、黑云母(3%)。基质中长石也大多蚀变为粘土矿物。石英斑岩呈浅灰色—浅肉红色,斑状结构,块状构造。斑晶约占35%,主要为石英(25%)、钾长石(4%)、斜长石(3%)、黑云母(3%)。钾长石强烈泥化,表面呈尘土状;黑云母多蚀变为绿帘石和绿泥石。基质为隐晶质结构。

4　分析测试方法

此次分析的2件锆石分别选自魏家钨矿区祥林铺岩体花岗斑岩(XLP−1)和石英斑岩(XLP−2)。先将样品粉碎至80~100目,用常规浮选和电磁选方法进行分选,然后在双目镜下挑选晶型完好,透明度好的锆石颗粒,将这些具有代表性的锆石颗粒固定

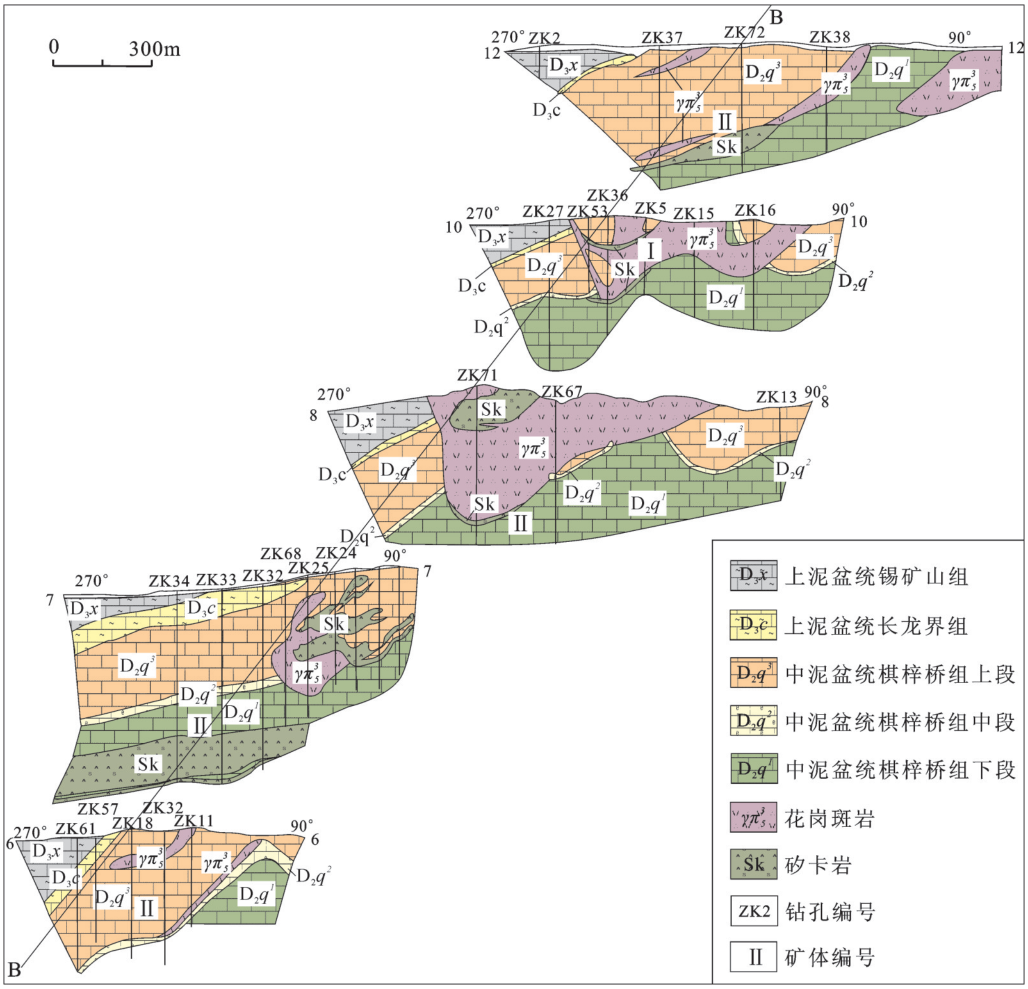

图3　魏家钨矿床矿体分布图(据文献[3]修改)

Fig.3 The distribution of tungsten orebodies in the Weijia W deposit (modified after reference [3])

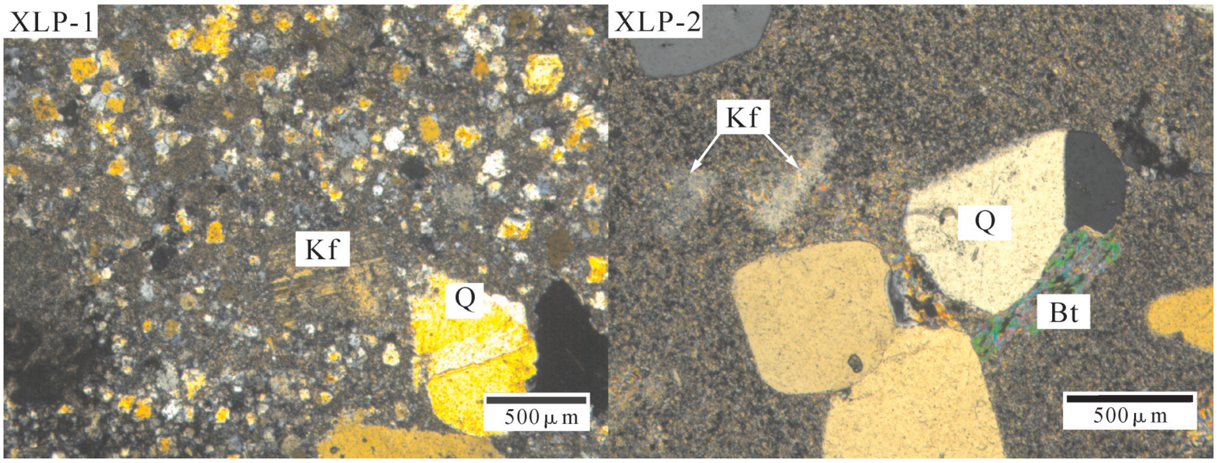

图4　祥林铺岩体显微照片(正交偏光)

Q—石英; Kf—钾长石; Bt—黑云母

Fig.4 Photomicrographs of the Xianglinpu granites (crossed nicols)

Q−Quartz; Kf−K−feldspar; Bt−Biotite

在无色透明的环氧树脂表面并对其表面抛光使锆石暴露以待测试。在镜下对锆石样品进行透射光和反射光显微照相，并用阴极发光扫描电镜进行图像分析，观察锆石形态特征，选出具有明显韵律环带结构且无裂纹的岩浆锆石(图5)进行测试。

锆石U−Pb定年测试在中国地质科学院矿产资源研究所MC−ICP−MS实验室完成，锆石定年分析所用仪器为Finnigan Neptune型MC−ICP−MS及与之配套的Newwave UP 123激光剥蚀系统。激光剥蚀所用的斑束直径为25 μm，频率为10 Hz，能量密度约为2.5 J/cm^2，以He为载气。信号较小的^{207}Pb、^{206}Pb、$^{204}Pb(+^{204}Hg)$和^{202}Hg用离子计数器接受，^{208}Pb、^{232}Th、^{238}U信号用法拉第杯接受，实现了所有目标同位素信号的同时接收并且不同质量数的峰基本上都是平坦的，进而可以获得高精度的数据，均匀锆石颗粒$^{207}Pb/^{206}Pb$、$^{206}Pb/^{238}U$、$^{207}Pb/^{235}U$的测试精度(2σ)均为2%左右。LA−MC−ICP−MS激光剥蚀采样采用单点剥蚀的方法，数据分析前用锆石GJ−1调试仪器，使之达到最优状态，锆石U−Pb定年以锆石GJ−1为外标，U、Th含量以锆石M127(U 923×10^{-6}、Th 439×10^{-6}、Th/U 0.475[11])为外标进行校正。在测试过程中每测定10个样品前后重复测定2个锆石GJ−1对样品进行校正，并测量1个锆石标样Plesovice，观察仪器的状态以保证测试的精确度。数据处理采用ICPMSDaTaCal4.3程序[12]，测量过程中绝大多数分析点$^{206}Pb/^{204}Pb$>500，故不进行普通铅校正，^{204}Pb由离子计数器检测，^{204}Pb含量异常高的分析点可能受包体等普通铅影响，对^{204}Pb含量异常高的分析点在计算时剔除，锆石年龄谐和图用Isoplot3.0程序获得。详细实验测试过程可参见侯可军等(2009)[13]。

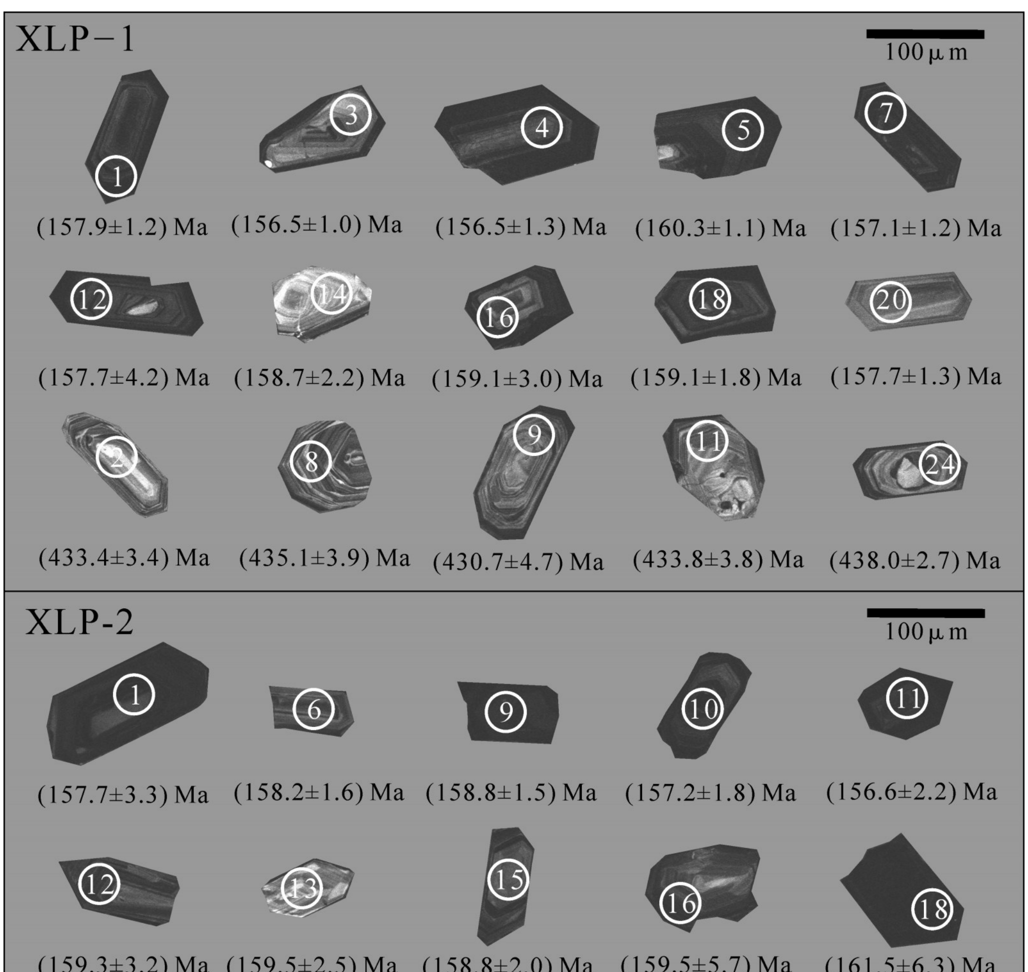

图5 祥林铺岩体代表性锆石CL图
Fig.5 CL images of representative zircons from the Xianglinpu granites

5 分析结果

魏家钨矿区祥林铺岩体中挑选出的锆石大部分为无色，部分略带浅黄色。阴极发光图像(图5)显示锆石颗粒多为半自形−自形，呈短柱状或长柱状，长度为60~160 μm，长宽比多介于1∶1.2~1∶3，裂隙少，大部分具有密集而清晰的震荡环带。LA−MC−ICP−MS锆石U−Pb测年结果(表1)表明，绝大部分锆石Th/U大于0.3，具有典型岩浆锆石特征[14−15]。对矿区内花岗斑岩(XLP−1)进行的15个有效测点中，有10个测点$^{206}Pb/^{238}U$年龄集中在156.4~160.3 Ma，加权平均值为(157.8±0.9) Ma，MSWD=1.06(图6)，在一致曲线图中10个数据点都分布在谐和线上及其附近，年龄比较集中，谐和度较高，可以代表岩体的形成年龄，指示矿区内花岗斑岩的侵位时代约为158 Ma；另外5个有效测点$^{206}Pb/^{238}U$年龄集中于430.7~438.0 Ma，加权平均值为(435.0±3.1) Ma，MSWD=0.6，指示花岗岩浆上升过程中捕获加里东期的岩浆锆石(435 Ma)。对矿区内石英斑岩(XLP−2)进行的10个有效测点的$^{206}Pb/^{238}U$年龄集中于156.6~161.5 Ma，加权平均值为(158.3±1.4) Ma，MSWD=0.2(图6)，可代表矿区内石英斑岩的侵位年龄。

6 讨 论

6.1 花岗岩形成时代的厘定及其指示意义

本次锆石U−Pb测年结果显示，祥林铺岩体花岗斑岩侵位年龄为(157.8±0.9) Ma，石英斑岩的侵位年龄为(158.3±1.4) Ma，二者在测试误差范围内一致，表明祥林铺岩体的侵位年龄约为158 Ma。花岗岩与矿体的接触关系显示，矽卡岩化和大理岩化等蚀变主要围绕祥林铺花岗岩分布(图2)，钻孔资料也显示魏家钨矿床矿体主要赋存于祥林铺花岗斑岩内及其与中泥盆统棋梓桥组碳酸盐岩接触带的矽卡岩中(图3)，矿体形态及分布主要受岩体与围岩的接触带控制[2−3]，因而魏家矽卡岩型钨矿床在空间上与祥林铺花岗斑岩密切相关，二者在时间及成因上亦应密切相关。考虑到全球主要的矽卡岩型矿床的形成与成矿岩体的侵位在误差范围内基本一致[16]，因而可以认为魏家钨矿区的成矿作用与矿区花岗岩的侵位近于同时，二者均形成于晚侏罗世(158 Ma左右)。结合区域上已有的高精度成岩成矿年龄数据，南岭地区主要钨锡多金属矿床的成岩成矿作用主要集中于160~150 Ma[17−39]，魏家钨矿应属于南岭地区中晚侏罗世“大规模成矿”作用的重要组成部分。另外，祥林铺岩体花岗斑岩中捕获的加里东期的岩浆锆石记录了该区发生过加里东期的岩浆事件，矿区深部可能存在加里东期岩浆岩，这与华南地区广泛存在加里东期构造岩浆活动的地质事实相吻合[40−44]。最近，杨振等(2014)报道了相邻的都庞岭地区新发现的牛塘界钨矿的成岩成矿作用主要集中于约420 Ma [43]，与本次研究的魏家钨矿区花岗斑岩中捕获的加里东期锆石年龄接近，这对于该区寻找加里东期花岗岩及相关钨矿给予了重要启示。

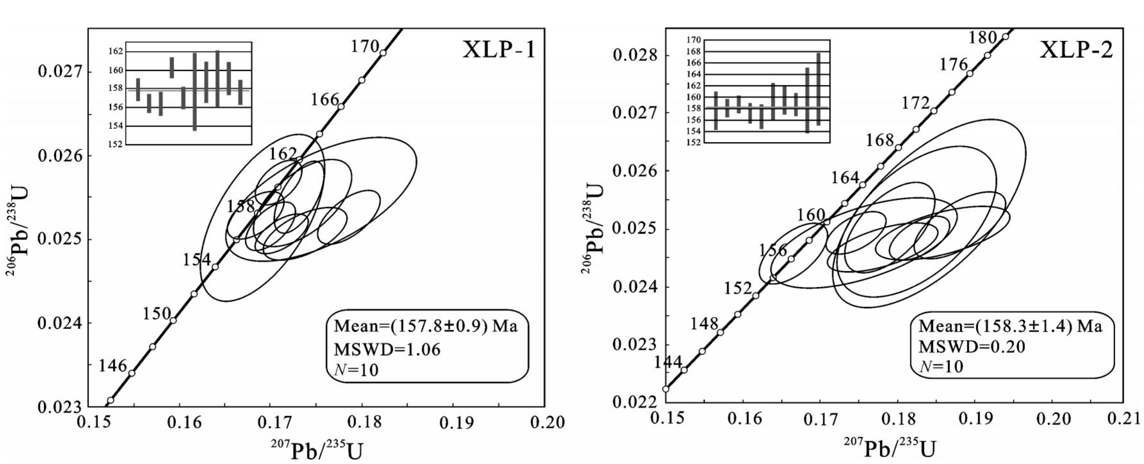

图6 魏家钨矿区祥林铺岩体锆石U−Pb一致曲线图
Fig.6 U−Pb concordia diagrams of zircons from Xianglinpu granites

表1 祥林铺岩体花岗斑岩锆石LA−MC−ICP−MS U−Pb年代学测试结果

Table 1 LA−MC−ICP−MS U−Pb isotopic compositions of zircons for the Xianglinpu granite porphyry

测点号	含量/10^{-6}			同位素比值									年龄 t/Ma			
	Pb	Th	U	$^{207}Pb/^{206}Pb$	1σ	$^{207}Pb/^{235}U$	1σ	$^{206}Pb/^{238}U$	1σ	$^{208}Pb/^{232}Th$	1σ	Th/U	$^{207}Pb/^{206}Pb$	$^{207}Pb/^{235}U$	$^{206}Pb/^{238}U$	$^{208}Pb/^{232}Th$
XLP−1−1	487	940	1950	0.0494	0.0003	0.1683	0.0020	0.0248	0.0002	0.0019	0.0002	0.4822	168.6±17.6	158.0±1.7	157.9±1.2	39.0±4.8
XLP−1−2	562	429	403	0.0563	0.0005	0.5378	0.0070	0.0695	0.0006	0.0052	0.0006	1.0658	464.9±13.9	437.0±4.6	433.4±3.4	104.2±12.2
XLP−1−3	114	220	498	0.0508	0.0005	0.1712	0.0020	0.0246	0.0002	0.0021	0.0002	0.4422	231.6±22.2	160.4±1.7	156.5±1.0	41.5±4.9
XLP−1−4	114	266	483	0.0515	0.0007	0.1738	0.0030	0.0246	0.0002	0.0017	0.0002	0.5504	261.2±31.5	162.7±2.6	156.5±1.3	33.5±4.6
XLP−1−5	194	428	1546	0.0494	0.0003	0.1708	0.0017	0.0252	0.0002	0.0017	0.0002	0.2765	168.6±17.6	160.1±1.5	160.3±1.1	33.8±3.5
XLP−1−7	564	1299	2192	0.0502	0.0003	0.1699	0.0018	0.0247	0.0002	0.0017	0.0002	0.5927	211.2±13.0	159.3±1.6	157.1±1.2	35.1±3.6
XLP−1−8	717	578	888	0.0573	0.0003	0.5489	0.0065	0.0698	0.0006	0.0050	0.0005	0.6504	501.9±17.6	444.3±4.2	435.1±3.9	100.2±11.0
XLP−1−9	596	506	747	0.0562	0.0004	0.5326	0.0073	0.0691	0.0008	0.0048	0.0006	0.6771	457.5±16.7	433.6±4.8	430.7±4.7	96.3±11.4
XLP−1−11	438	365	515	0.0557	0.0004	0.5326	0.0066	0.0696	0.0006	0.0047	0.0006	0.7094	438.9±10.2	433.6±4.4	433.8±3.8	94.1±11.5
XLP−1−12	268	497	1271	0.0497	0.0009	0.1690	0.0044	0.0248	0.0007	0.0020	0.0003	0.3907	189.0±16.7	158.6±3.8	157.7±4.2	40.9±5.4
XLP−1−14	252	439	721	0.0507	0.0009	0.1735	0.0035	0.0249	0.0004	0.0021	0.0003	0.6093	233.4±72.2	162.5±3.1	158.7±2.2	42.0±5.3
XLP−1−16	49	91	110	0.0512	0.0022	0.1756	0.0069	0.0250	0.0005	0.0024	0.0004	0.8227	250.1±98.1	164.3±5.9	159.1±3.0	48.9±8.5
XLP−1−18	626	1251	2047	0.0504	0.0003	0.1732	0.0019	0.0250	0.0003	0.0017	0.0002	0.6110	213.0±14.8	162.2±1.6	159.1±1.8	33.4±4.4
XLP−1−20	114	197	408	0.0524	0.0005	0.1786	0.0023	0.0248	0.0002	0.0020	0.0003	0.4834	301.9±20.4	166.8±2.0	157.7±1.3	39.7±6.5
XLP−1−24	218	143	270	0.0582	0.0003	0.5631	0.0040	0.0703	0.0004	0.0062	0.0005	0.5277	600.0±11.1	453.6±2.6	438.0±2.7	124.5±10.2

表2 祥林铺岩体石英斑岩锆石LA−MC−ICP−MS U−Pb年代学测试结果

Table 2 LA−MC−ICP−MS U−Pb isotopic compositions of zircons for the Xianglinpu quartz porphyry

测点号	含量/10^{-6}			同位素比值									年龄 t/Ma			
	Pb	Th	U	$^{207}Pb/^{206}Pb$	1σ	$^{207}Pb/^{235}U$	1σ	$^{206}Pb/^{238}U$	1σ	$^{208}Pb/^{232}Th$	1σ	Th/U	$^{207}Pb/^{206}Pb$	$^{207}Pb/^{235}U$	$^{206}Pb/^{238}U$	$^{208}Pb/^{232}Th$
XLP-2-1	77	168	543	0.0516	0.0033	0.1757	0.0079	0.0248	0.0005	0.0019	0.0011	0.3087	333.4±143.5	164.4±6.8	157.7±3.3	39.2±22.4
XLP-2-6	116	194	601	0.0535	0.0004	0.1828	0.0027	0.0248	0.0003	0.0020	0.0003	0.3224	350.1±12.0	170.5±2.3	158.2±1.6	40.5±7.0
XLP-2-9	406	696	1661	0.0510	0.0004	0.1747	0.0026	0.0249	0.0002	0.0015	0.0003	0.4191	242.7±12.0	163.5±2.2	158.8±1.5	30.9±6.1
XLP-2-10	68	95	108	0.0526	0.0012	0.1781	0.0046	0.0247	0.0003	0.0024	0.0006	0.8759	322.3±50.0	166.4±4.0	157.2±1.8	49.0±11.7
XLP-2-11	241	469	754	0.0494	0.0005	0.1665	0.0030	0.0246	0.0003	0.0014	0.0003	0.6223	164.9±22.2	156.4±2.6	156.6±2.2	28.4±5.5
XLP-2-12	385	713	1589	0.0521	0.0005	0.1789	0.0039	0.0250	0.0005	0.0015	0.0003	0.4483	300.1±5.6	167.1±3.4	159.3±3.2	31.1±5.3
XLP-2-13	185	360	513	0.0546	0.0007	0.1881	0.0040	0.0251	0.0004	0.0016	0.0003	0.7019	398.2±32.4	175.0±3.4	159.5±2.5	31.8±5.4
XLP-2-15	29	70	82	0.0541	0.0013	0.1858	0.0057	0.0249	0.0003	0.0018	0.0004	0.8539	376.0±53.7	173.0±4.9	158.8±2.0	36.0±8.7
XLP-2-16	23	136	178	0.0530	0.0039	0.1821	0.0069	0.0250	0.0009	0.0016	0.0000	0.7683	327.8±166.6	169.9±6.0	159.5±5.7	32.0±0.0
XLP-2-18	215	523	436	0.0529	0.0017	0.1844	0.0082	0.0254	0.0010	0.0017	0.0003	1.1983	324.1±69.4	171.9±7.1	161.5±6.3	35.3±5.6

6.2 魏家钨矿的发现对于南岭西段钨成矿作用及找矿勘查的指示

南岭地区中生代发育大规模的花岗质岩浆作用并伴随有巨量钨锡多金属元素的堆积成矿，是中国东部中生代大规模成矿作用的重要组成部分[45, 46]。然而，以往对南岭地区钨锡矿床时空分布格局的研究有不同的认识，其原因在于不同学者对于南岭地区所包括的范围划分不同。以往对整个华南地区钨锡矿的研究中，许多学者将右江盆地周缘发育的一系列锡多金属矿床(如个旧、大厂等)也划分到南岭的范围，构成了广义的“南岭钨锡成矿带”，使得钨锡矿床在空间分布上呈现“东钨西锡”的分布格局[47]。事实上，传统认为南岭地区是指武夷山以西和越城岭以东地带(东经111°~116°，北纬27°~24°)，包括赣南、湘南、粤北和桂东地区[21]；近年来积累的高精度成岩成矿年代学数据显示，右江盆地周缘的锡多金属矿床主要形成于中晚白垩世(100~80 Ma)[48, 49]，与南岭地区钨锡矿床主要形成于中晚侏罗世(160~150 Ma)明显不同，地理上也处于“南岭”以西[27, 50]，因而二者应为不同地球动力学背景之下不同成岩成矿事件的产物。

从南岭地区以往发现的中晚侏罗世钨锡矿床的空间分布上来看，东部赣南粤北地区主要以石英脉型钨多金属矿床为主，锡资源量很少；湘南的千里山—骑田岭一带广泛发育矽卡岩型矿床，从金属量上呈现钨锡并重的格局；往西花山—姑婆山、九嶷山以及都庞岭地区已发现的矿床主要以锡为主，而在都庞岭地区新近发现的牛塘界钨矿则为加里东期成矿事件的产物[43]。以往的高精度同位素年代学数据显示，南岭地区中晚侏罗世的钨锡矿床整体上呈现“东钨、西锡、中段钨锡并重”的格局。然而，本研究获得与魏家超大型矽卡岩型钨矿密切相关的祥林铺岩体的成岩年龄约为158 Ma，表明南岭西端中晚侏罗世同样存在大规模的钨成矿作用。结合南岭中东段中晚侏罗世钨矿床的大量分布，我们认为南岭地区中晚侏罗世的钨成矿作用贯穿整个南岭地区；另外，魏家超大型矽卡岩型钨矿床成岩成矿时代的厘定，指示了南岭西端不仅是中晚侏罗世锡成矿作用的有利部位，同样也是晚侏罗世钨多金属矿床的找矿勘查的有利地段。

7 结 论

(1) 湘南祥林铺岩体花岗斑岩和石英斑岩的锆

石LA−MC−ICP−MS U−Pb年龄分别为(157.8±0.9) Ma和(158.3±1.4) Ma, 指示魏家钨矿区成岩成矿作用主要发生在晚侏罗世(约158 Ma), 与南岭地区中生代大规模W−Sn多金属矿床成矿时限(160~150 Ma)一致。

(2) 祥林铺花岗斑岩捕获有加里东期岩浆锆石(435 Ma), 指示该区发生过加里东期的岩浆事件, 这与华南地区广泛存在加里东期构造运动及相关的岩浆活动的地质事实吻合。

(3) 魏家钨矿成岩成矿时代的厘定, 指示了南岭西端不仅是中晚侏罗世锡成矿作用的有利部位, 同样也是晚侏罗世钨多金属矿床找矿勘查的有利地段。

致谢: 湖南地质勘察院张怡军高级工程师和中国地质科学院侯可军博士分别在野外样品采集和锆石同位素分析过程中提供了指导和帮助; 资料收集和成文过程中得到了中国地质大学(北京)轩一撒、弥佳茹的帮助; 审稿专家及责任编辑杨艳老师提出了许多建设性的意见; 在此一并表示感谢。

参考文献(References):

[1] 袁顺达, 王旭东. 湘南魏家钨矿区祥林铺岩体的锆石LA−(MC)−ICP−MS U−Pb测年及其意义[J]. 地质学报, 2013, 87: 62−64.
Yuan Shunda, Wang Xudong. Zircon LA−MC−ICP−MS U−Pb dating of the Xianglinpu granites from Weijia tungsten deposit in southern Hunan Province and its geological significance[J]. Acta Geological Sinica, 2013, 87: 62−64(in Chinese).

[2] 李福顺, 康如华, 胡绪云, 等. 南岭魏家钨矿床地质特征及找矿前景分析[J]. 中国地质, 2012, 39(2): 445−457.
Li Fushun, Kang Ruhua, Hu Xuyun, et al. Geological characteristics and ore−search prospect of the Weijia tungsten deposit in Nanling region[J]. Geology in China, 2012, 39(2): 445−457(in Chinese with English abstract).

[3] 杨冲, 申志军, 匡文龙, 等. 湘西南铜山岭地区钨多金属矿床地质特征及成矿机制探讨——以祥霖铺矿床为例[J]. 地质找矿论丛, 2012, 27(2): 156−161.
Yang Chong, Shen Zhijun, Kuang Wenlong, et al. The geological features and minerogenetic mechanism of tungsten−polymetallic deposits in Tongshanling area, Southwestern Hunan: Taking Xianglinpu deposit as an example[J]. Contributions to Geological and Mineral Resources Research, 2012, 27(2): 156−161(in Chinese with English abstract).

[4] Gilder S A, Gill J, Coe R S, et al. Isotopic and paleomagnetic constraints on the Mesozoic tectonic evolution of South China[J]. Journal of Geophysical Research (B), 1996, 101(7): 16137−16155.

[5] 毛景文, 谢桂青, 郭春丽, 等. 华南地区中生代主要金属矿床时空分布规律和成矿环境[J]. 高校地质学报, 2008, 14(4): 510−526.
Mao Jingwen, Xie Guiqing, Guo Chunli, et al. Spatial−temporal distribution of Mesozoic ore deposits in South China and their metallogenic settings[J]. Geological Journal of China Universities, 2008, 14(4): 510−526 (in Chinese with English abstract).

[6] 毛景文, 谢桂青, 程彦博, 等. 华南地区中生代主要金属矿床模型[J]. 地质论评, 2009, 55(3): 347−354.
Mao Jingwen, Xie Guiqing, Cheng Yanbo, et al. Mineral deposit models of Mesozoic ore deposits in South China[J]. Geological Review, 2009, 55(3): 347−354(in Chinese with English abstract).

[7] 彭建堂, 胡瑞忠, 袁顺达, 等. 湘南中生代花岗质岩石成岩成矿的时限[J]. 地质论评, 2008, 54(5): 617−625.
Peng Jiantang, Hu Ruizhong, Yuan Shunda, et al. The time ranges of granitoid emplacement and related nonferrous metallic mineralization in southern Hunan[J]. Geological Review, 2008, 54 (5): 617−625(in Chinese with English abstract).

[8] Yuan S D, Mao J W, Cook N J, et al. A Late Cretaceous tin metallogenic event in Nanling W−Sn metallogenic province: Constraints from U−Pb, Ar−Ar geochronology at the Jiepailing Sn−Be−F deposit, Hunan, China[J]. Ore Geology Reviews, 2015, 65: 283−293.

[9] 张怡军, 黄光华, 尚立晓, 等. 湘南地区钨矿成矿地质特征[J]. 中国地质, 2014, 41(1): 246−255.
Zhang Yijun, Huang Guanghua, Shang Lixiao, et al. Geological characteristics of tungsten deposits in southern Hunan[J]. Geology in China, 2014, 41(1): 246−255(in Chinese with English abstract).

[10] 葛肖虹, 刘俊来, 任收麦, 等. 中国东部中—新生代大陆构造的形成与演化[J]. 中国地质, 2014, 41(1): 19−38.
Ge Xiaohong, Liu Junlai, Ren Shoumai, et al. The formation and evolution of the Mesozoic−Cenozoic continental tectonics in eastern China[J]. Geology in China, 2014, 41(1): 19−38(in Chinese with English abstract).

[11] Nasdala L, Hofmeister W, Norberg N, et al. Zircon M257: A homogeneous natural reference material for the ion microprobe U−Pb analysis of zircon [J]. Geostandards and Geoanalytical Research, 2008, 32: 247−265.

[12] Liu Y S, Hu Z C, Gao S, et al. In situ analysis of major and trace elements of anhydrous minerals by LA−ICP−MS without applying an internal standard[J]. Chemical Geology, 2008, 257: 34−43.

[13] 侯可军, 李延河, 田有荣. LA−MC−ICP−MS锆石微区原位U−Pb定年技术[J]. 矿床地质, 2009, 28(4): 481−492.
Hou Kejun, Li Yanhe, Tian Yourong. In situ U−Pb zircon dating using laser ablation−multi ion couting−ICP−MS[J]. Mineral Deposits, 2009, 28(4): 481−492(in Chinese with English abstract).

[14] Hoskin P W O, Schaltegger U. The composition of zircon and igneous and metamorphic petrogenesis[C]//Hanchar J M, Hoskin P W O(eds.). Zircon: Reviews in Mineralogy and Geochemistry, 2003, 53: 27−62.

[15] Toscano M, Pascual E, Nesbitt R W, et al. Geochemical discrimination of hydrothermal and igneous zircon in the Iberian Pyrite Belt Spain[J]. Ore Geology Reviews, 2014, 56: 301−311.

[16] Meinert L D. Skarns and skarn deposits[J]. Geoscience Canada, 1992, 19(4): 145−162.

[17] 李红艳, 毛景文, 孙亚莉, 等. 柿竹园钨多金属矿床的Re−Os同位素等时线年龄研究[J]. 地质论评, 1996, 42(3): 261−267.
Li Hongyan, Mao Jingwen, Sun Yali, et al. Re− Os isotopic chronology of molybdenites in the Shizhuyuan polymetallic tungsten deposit, southern Hunan[J]. Geological Review, 1996, 42(3): 261−267(Chinese with English abstract).

[18] Li X H, Liu D Y, Sun M, et al. Precise Sm−Nd and U−Pb isotopic dating of the supergiant Shizhuyuan polymetallic deposit and its host granite, SE China[J]. Geological Magazine, 2004, 141(2): 225−231.

[19] 毛景文, 李晓峰, Lehmann B, 等. 湖南芙蓉锡矿床锡矿石和有关花岗岩的 $^{40}Ar-^{39}Ar$ 年龄及其地球动力学意义[J]. 矿床地质, 2004, 23(2): 164−175.
Mao Jingwen, Li Xiaofeng, Lehmann B, et al. $^{40}Ar-^{39}Ar$ dating of tin ores and related granite in Furong tin orefield, Hunan Province, and its geodynamic significance[J]. Mineral Deposits, 2004, 23(2): 164−175(in Chinese with English abstract).

[20] 毛景文, 谢桂青, 李晓峰, 等. 华南地区中生代大规模成矿作用与岩石圈多阶段伸展[J]. 地学前缘, 2004, 11(1): 45−55.
Mao Jingwen, Xie Guiqing, Li Xiaofeng, et al. Mesozoic large scale mineralization and multiple lithospheric extension in South China[J]. Earth Science Froniters, 2004, 11(1): 45−56(in Chinese with English abstract).

[21] 毛景文, 谢桂青, 郭春丽, 等. 南岭地区大规模钨锡多金属成矿作用: 成矿时限及地球动力学背景[J]. 岩石学报, 2007, 23(10): 2329−2338.
Mao Jingwen, Xie Guiqing, Guo Chunli, et al. Large− scale tungsten− tin mineralization in the Nanling region, South China: Metallogenic ages and corresponding geodynamic processes[J]. Acta Petrologica Sinica, 2007, 23(10): 2329− 2338 (in Chinese with English abstract).

[22] Peng J T, Zhou M F, Hu R Z, et al. Precise molybdenite Re−Os and mica Ar− Ar dating of the Mesozoic Yaogangxian tungsten deposit, central Nanling district, South China[J]. Mineralium Deposita, 2006, 41(7): 661−669.

[23] 陈毓川, 王登红, 徐志刚, 等. 华南区域成矿和中生代岩浆成矿规律概要[J]. 大地构造与成矿学, 2014, 38(2): 219−229.
Chen Yuchuan, Wang Denghong, Xu Zhigang, et al. Outline of regional metallogeny of ore deposits associateed with the Mesozoic magmatism in South China[J]. Geotectonica et Metallogenia, 2014, 38(2): 219− 229(in Chinese with English abstract).

[24] Yuan S D, Peng J T, Shen N P, et al. $^{40}Ar-^{39}Ar$ isotopic dating of the Xianghualing Sn− polymetallic orefield in Southern Hunan, China and its geological implication[J]. Acta Geologica Sinica, 2007, 81: 278−286.

[25] Yuan S D, Peng J T, Hu R Z, et al. A precise U− Pb age on cassiterite from the Xianghualing tin− polymetallic deposit (Hunan), South China[J]. Mineralium Deposita, 2008, 43(4): 375−382.

[26] Yuan S D, Peng J T, Hao S, et al. In situ LA−MC−ICP−MS and ID−TIMS U−Pb geochronology of cassiterite in the giant Furong tin deposit, Hunan Province, South China: New constraints on the timing of tin− polymetallic mineralization[J]. Ore Geology Reviews, 2011, 43(1): 235−242.

[27] 华仁民, 李光来, 张文兰, 等. 华南钨和锡大规模成矿作用的差异及其原因初探[J]. 矿床地质, 2010, 29(1): 9−23.
Hua Renmin, Li Guanglai, Zhang Wenlan, et al. A tentative discussion on differences between large− scale tungsten and tin mineralizations in South China[J]. Mineral Deposits, 2010, 29(1): 2−23(in Chinese with English abstract).

[28] 李顺庭, 王京彬, 祝新友, 等. 湖南瑶岗仙复式岩体的年代学特征[J]. 地质与勘探, 2011, 47(2): 143−150.
Li Shunting, Wang Jingbin, Zhu Xinyou, et al. Chronological characteristics of the Yaogangxian composite pluton in Hunan Province[J]. Geology and Exploration, 2011, 47(2): 143− 150(in Chinese with English abstract).

[29] Mao J W, Chen M H, Yuan S D, et al. Geological characteristics of the Qinhang Metallogenic Belt in South China and spatial− temporal distribution regularity of mineral deposits [J]. Acta Geologica Sinica, 2011, 85(5): 636−657.

[30] 刘晓菲, 袁顺达, 吴胜华. 湖南金船塘锡铋矿床辉钼矿 Re−Os同位素测年及其地质意义[J]. 岩石学报, 2012, 28(1): 39−51.
Liu Xiaofei, Yuan Shunda, Wu Shenghua. Re− Os dating of the molybdenite from the Jinchuantang tin−bismuth deposit in Hunan Province and its geological significance[J]. Acta Petrologica Sinica, 2012, 28(1): 39−51(in Chinese with English abstract).

[31] 袁顺达, 刘晓菲, 王旭东, 等. 湘南红旗岭锡多金属矿床地质特征及 Ar−Ar 同位素年代学研究[J]. 岩石学报, 2012, 28(12): 3788−3797.
Yuan Shunda, Liu Xiaofei, Wang Xudong, et al. Geological characteristics and $^{40}Ar-^{39}Ar$ geochronology of the Hongqiling tin deposit in southern Hunan Province[J]. Acta Petrologica Sinica, 2012, 28(2): 3787−3797(in Chinese with English abstract).

[32] 袁顺达, 张东亮, 双燕, 等. 湘南新田岭大型钨钼矿床辉钼矿 Re−Os 同位素测年及其地质意义[J]. 岩石学报, 2012, 28(1): 27−38.
Yuan Shunda, Zhang Dongliang, Shuang Yan, et al. Re−Os dating of molybdenite from the Xintianling giant tungsten−molybdenum deposit in southern Hunan Province, China and its geological implications[J]. Acta Petrologica Sinica, 2012, 28(1): 27− 38(in Chinese with English abstract).

[33] Wang Y J, Fan W M, Zhao G C, et al. Zircon U− Pb geochronology of gneissic rocks in the Yunkai massif and its implications on the Caledonian event in the South China Block[J]. Gondwana Research, 2007, 12: 404−416.

[34] 张芳荣, 舒良树, 王德滋, 等. 华南东段加里东期花岗岩类形成构造背景探讨[J]. 地学前缘, 2009, 16(1): 248−260.
Zhang Fangrong, Shu Liangshu, Wang Dezi, et al. Discussion on the tectonic setting of Caledonian granitoids in the eastern segment of South China[J]. Earth Science Frontiers, 2009, 16(1): 248−260(in Chinese with English abstract).

[35] Feng C Y, Zhao Z, Qu W J, et al. Temporal consistency between granite evolution and tungsten mineralization in Huamei’ao,

southern Jiangxi Province, China: Evidence from precise zircon U–Pb, molybdenite Re–Os, and muscovite $^{40}Ar-^{39}Ar$ isotope geochronology[J]. Ore Geology Reviews, 2015, 65: 1005−1020.

[36] Mao J W, Cheng Y B, Chen M H, et al. Major types and time-space distribution of Mesozoic ore deposits in South China and their geodynamic settings[J]. Mineralium Deposita, 2013, 48: 267−294.

[37] Li H, Watanabe K, Yonezu K. Zircon morphology, geochronology and trace element geochemistry of the granites from the Huangshaping polymetallic deposit, South China: Implications for the magmatic evolution and mineralization process[J]. Ore Geology Reviews, 2014, 60: 14−35.

[38] 马丽艳, 付建明, 伍式崇, 等. 相东锡田垄上锡多金属矿床 $^{40}Ar/^{39}Ar$ 同为素定年研究[J]. 中国地质, 2008, 35(4): 706−713.
Ma Liyan, Fu Jianming, Wu Shichong, et al. $^{40}Ar/^{39}Ar$ isotopic dating of the Longshang tin-polymetallic deposit, Xitian orefield, eastern Hunan[J]. Geology in China, 2008, 35(4): 706−713(in Chinese with English abstract).

[39] 陈迪, 陈焰明, 马爱军, 等. 湖南锡田岩体的岩浆混合成因: 岩相学、岩石地球化学和U−Pb年龄证据[J]. 中国地质, 2014, 41(1): 61−78.
Chen Di, Chen Yanming, Ma Aijun, et al. Magma mixing in the Xitian pluton of Hunan Province: Evidence from petrography, geochemistry and zircon U−Pb age[J]. Geology in China, 2014, 41 (1): 61−78(in Chinese with English abstract).

[40] 王彦斌, 王登红, 韩娟, 等. 湖南益将稀土−钪矿的石英闪长岩锆石U−Pb定年和Hf同位素特征: 湘南加里东期岩浆活动的年代学证据[J]. 中国地质, 2010, 37(4): 1062−1070.
Wang Yanbin, Wang Denghong, Han Juan, et al. U−Pb dating and Hf isotopic characteristics of zircons from quartz−diorite in the Yijiang REE−Sc deposit, Rucheng County, Hunan: Constraints on the timing of Caledonian magmatic activity in South China[J]. Geology in China, 2010, 37(4): 1062−1070(in Chinese with English abstract).

[41] 徐先兵, 张岳桥, 贾东, 等. 华南早中生代大地构造过程[J]. 中国地质, 2009, 36(3): 573−593.
Xu Xianbing, Zhang Yueqiao, Jia Dong, et al. Early Mesozoic geotectonic processes in South China[J]. Geology in China, 2009, 36(3): 573−593(in Chinese with English abstract).

[42] 王磊, 龙文国, 周岱. 云开地区加里东期花岗岩锆石U−Pb年龄及其地质意义[J]. 中国地质, 2013, 40(4): 1016−1029.
Wang Lei, Long Wenguo, Zhou Dai. Zircon LA−ICP−MS U−Pb age of Caledonian granites from Precambrian basement in Yunkai area and its geological implications[J]. Geology in China, 2013, 40 (4): 1016−1029(in Chinese with English abstract).

[43] 杨振, 王汝成, 张文兰, 等. 桂北牛塘界加里东期花岗岩及其矽卡岩型钨矿成矿作用研究[J]. 中国科学: 地球科学, 2014, 44(7): 1357−1373.
Yang Zhen, Wang Rucheng, Zhang Wenlan, et al. Skarn−type tungsten mineralization associated with the Caledonian (Silurian) Niutangjie granite, northern Guangxi, China[J]. Science China: Earth Sciences, 2014, 44(7): 1357−1373(in Chinese).

[44] 刘伟, 曾佐勋, 李绍凡, 等. 广西富川岩鹰嘴W−Mo−Cu多金属矿区斑岩体LA−ICP−MS锆石U−Pb定年及其地质意义[J]. 中国地质, 2014, 41(3): 797−813.
Liu Wei, Zeng Zuoxun, Li Shaofan, et al. LA−ICP−MS zircon U−Pb dating of the granitic and granodioritic porphyries from the Yanyingzui W−Mo−Cu polymetalic ore district in Fuchuan area, Guangxi, and its geological implications[J]. Geology in China, 2014, 41(3): 797−813(in Chinese with English abstract).

[45] 华仁民, 毛景文. 试论中国东部中生代成矿大爆发[J]. 矿床地质, 1999, 18(4): 300−308.
Hua Renmin, Mao Jingwen. A preliminary discussion on the Mesozoic metallogenic explosion in east China[J]. Mineral Deposits, 1999, 18(4): 300−308(in Chinese with English abstract).

[46] 毛景文, 华仁民, 李晓波. 浅议大规模成矿作用与大型矿集区[J]. 矿床地质, 1999, 18(4): 291−299.
Mao Jingwen, Hua Renmin, Li Xiaobo. A preliminary study of large− scale metallogenesis and large clusters of mineral deposits[J]. Mineral Deposits, 1999, 18(4): 291−299(in Chinese with English abstract).

[47] 李建康, 王登红, 梁婷, 等. 南岭区域成矿与深部探测的研究进展及其对西藏钨锡找矿的指示[J]. 地球学报, 2013, 34(1): 58−74.
Li Jiankang, Wang Denghong, Liang Ting, et al. Progress of research on metallogenic regularity and deep exploration in Nanling Region and its indication for W−Sn exploration in Tibet[J]. Acta Geoscientica Sinica, 2013, 34(1): 58−74(in Chinese with English abstract).

[48] 王登红, 陈毓川, 陈文, 等. 广西南丹大厂超大型锡多金属矿床的成矿时代[J]. 地质学报, 2004, 78(1): 132−138.
Wang Denghong, Chen Yuchuan, Chen Wen, et al. Dating the Dachang gaint tin−polymetallic deposit in Nandan, Guangxi[J]. Acta Geologica Sinica, 2004, 78(1): 132−138(in Chinese with English abstract).

[49] 杨宗喜, 毛景文, 陈懋弘, 等. 云南个旧老厂细脉带型锡矿白云母 $^{40}Ar-^{39}Ar$ 年龄及其地质意义[J]. 矿床地质, 2009, 28(3): 336−344.
Yang Zongxi, Mao Jingwen, Chen Maohong, et al. $^{40}Ar-^{39}Ar$ dating of muscovite from Laochang veinlet−like Sn deposit in Gejiu tin polymetallic ore district and its geological significance[J]. Mineral Deposits, 2009, 28(3): 336−344(in Chinese with English abstract).

[50] 华仁民, 陈培荣, 张文兰, 等. 论华南地区中生代3次大规模成矿作用[J]. 矿床地质, 2005, 24(2): 99−107.
Hua Renmin, Chen Peirong, Zhang Wenlan, et al. Three major metallogenic events in Mesozoic in South China[J]. Mineral Deposits, 2005, 24(2): 99−107(in Chinese with English abstract).